Amine–Amine Exchange in Aminium–Methanesulfonate Aerosols

ARTICLE *in* THE JOURNAL OF PHYSICAL CHEMISTRY C · DECEMBER 2014

Impact Factor: 4.77 · DOI: 10.1021/jp506560w

THE JOURNAL OF PHYSICAL CHEMISTRY C

Article

pubs.acs.org/JPCC

Amine−Amine Exchange in Aminium−Methanesulfonate Aerosols

Matthew L. Dawson,[†] Mychel E. Varner,[†] Véronique Perraud,[†] Michael J. Ezell,[†] Jacqueline Wilson,[‡] Alla Zelenyuk,[‡] R. Benny Gerber,*[,†,§,∥] and Barbara J. Finlayson-Pitts*[,†]

[†]Department of Chemistry, University of California, Irvine, California 92697-2025, United States

[‡]Physical Sciences Division, Pacific Northwest National Laboratory, Richland, Washington 99354, United States

[§]Institute of Chemistry, Fritz Haber Research Center, Hebrew University of Jerusalem, Jerusalem 91904, Israel

[∥]Laboratory of Physical Chemistry, University of Helsinki, FIN-00014 Helsinki, Finland

Supporting Information

ABSTRACT: Aerosol particles are ubiquitous in the atmosphere and have been shown to impact the Earth's climate, reduce visibility, and adversely affect human health. Modeling the evolution of aerosol systems requires an understanding of the species and mechanisms involved in particle growth, including the complex interactions between particle- and gas-phase species. Here we report studies of displacement of amines (methylamine, dimethylamine, or trimethylamine) in methanesulfonate salt particles by exposure to a different gas-phase amine, using a single particle mass spectrometer, SPLAT II. The variation of the displacement with the nature of the amine suggests that behavior is dependent on water in or on the particles. Small clusters of methanesulfonic acid with amines are used as a model in quantum chemical calculations to identify key structural elements that are expected to influence water uptake, and hence the efficiency of displacement by gas-phase molecules in the aminium salts. Such molecular-level understanding of the processes affecting the ability of gas-phase amines to displace particle-phase aminium species is important for modeling the growth of particles and their impacts in the atmosphere.

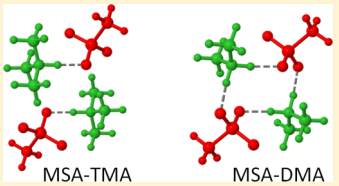

INTRODUCTION

Particulate matter is ubiquitous in the atmosphere and varies both temporally and spatially in size, concentration and composition. It affects visibility[1] and has been shown to have serious impacts on human health.[2−6] Particles can serve as condensation nuclei for clouds (CCN), which scatter and absorb incoming sunlight, thereby affecting the net solar radiation reaching the Earth's surface.[7,8] However, the ability of aerosol particles to act as CCN is dependent on their size and composition, making this a challenging system to model.[9] Indeed, the effect of aerosol particles on radiative forcing remains the largest uncertainty in predicting climate change.[8] A critical issue is the particle composition and its variation due to interaction with gases.

Sulfuric acid is a key species in new particle formation, although other species such as organics may also contribute.[7,10−13] From these small sizes, particles are subject to growth from a variety of gas-phase condensing species.[11,12,14] Methanesulfonic acid (MSA; Me_3SO_3H) is another significant component of atmospheric aerosols[15−23] and has been observed to be enhanced relative to sulfuric acid in particles <100 nm in diameter.[15,22,23] MSA is formed alongside sulfuric acid in the oxidation of organosulfur compounds such as dimethyl sulfide (DMS) and methyl mercaptan.[7,24−33] These reduced-sulfur species are emitted primarily from biological activity in the oceans,[34−39] with DMS alone accounting for about half of the natural sulfur emissions globally.[38,39] In addition, there are inland sources of reduced sulfur compounds[40−45] and indications of as-yet unidentified sources of atmospheric MSA.[19,46] While MSA has been proposed to primarily contribute to particle growth in the atmosphere,[47−49] there is evidence that MSA can also contribute to new particle formation.[50]

There is a great deal of evidence that amines and ammonia, which have a wide variety of both natural and anthropogenic sources,[51−53] play important roles in new particle formation and growth with sulfuric as well as methanesulfonic acid.[12,13,50,54−62] The largest source of atmospheric ammonia in the U.S. is livestock emissions, but industrial sources, fertilizers, soil, and vehicle emissions also contribute.[52] For amines, important sources include agriculture operations,[45,63−68] coal,[69] and biomass[70] burning, and more recently introduced sources such as carbon capture and storage devices.[71−74]

Despite much lower ambient concentrations, amines are thought to be comparable to ammonia in their contribution to particle formation and growth,[13,55,57,59,62,75,76] in part because of efficient displacement of the ammonium ion in particles by amines taken up from the gas phase.[77−85] Thus, methylamine (MA; $MeNH_2$), dimethylamine (DMA; Me_2NH) and trimethylamine (TMA; Me_3N) have been shown to efficiently displace NH_4^+ in ammonium-containing sulfate and nitrate particles over a range of particle sizes and relative humidity (RH). The studies to date show that phase plays an important

Special Issue: John C. Hemminger Festschrift

Received: July 1, 2014
Revised: August 21, 2014

   dx.doi.org/10.1021/jp506560w | J. Phys. Chem. C XXXX, XXX, XXX−XXX

role, with almost complete displacement occurring for aqueous particles, while it is incomplete for crystalline solids where diffusion is slow.[80,81] Consistent with this, displacement of ammonium in ammonium bisulfate clusters by DMA was shown to be size dependent, indicating that the salt core is more difficult for incoming DMA to penetrate.[79]

The displacement of ammonium ions by DMA in methanesulfonate clusters has been shown to occur with a reaction probability of ~1.[78] However, to our knowledge, an exploration of amine−amine (as opposed to ammonia-amine) exchange has not been reported in the literature for any salts, including those from MSA. If there are species-specific effects of condensed-phase amines on the physical properties of particles, it could have implications for further growth, and make amine−amine exchange reactions a potentially important atmospheric process. Here we report displacement experiments on particles containing MSA and amines using the single particle mass spectrometer, SPLAT II. The presence of water is shown to affect particle phase and the extent of displacement of the amine initially in the particle. To provide molecular level insight into the results, quantum chemical calculations were carried out for some representative MSA-amine clusters. We are especially delighted to contribute this paper to the Festschrift in honor of John Hemminger, a long-time colleague, collaborator and friend. John has been at the forefront of applying fundamental surface science techniques to problems of atmospheric importance, and integrating theory and experiment to provide unique molecular insights into the chemistry of complex systems. The studies reported here represent another example of the strength of such integration.

EXPERIMENTAL AND THEORETICAL METHODS

Amine−amine displacement experiments were performed at Pacific Northwest National Lab's Environmental Molecular Sciences Laboratory User Facility using SPLAT II operated in positive ion mode without a diffusion drier (to minimize contamination issues). All experiments were performed in 100 L Teflon chambers with gas- and particle-phase species diluted with zero air (OXARC; 19.5−20% O_2, 80−80.5% N_2, <1 ppm of CO, <1 ppm of CO_2, <0.5 ppm THC, <0.3 ppm of H_2O). Particle size distributions were monitored using a scanning mobility particle sizer (SMPS) consisting of a classifier (Model 3080; TSI), a differential mobility analyzer (Model 3081; TSI) and a condensation particle counter (Model 3786; TSI) operated with 0.3 L min^{-1} sample flow and 3.0 L min^{-1} sheath flow.

SPLAT II is a single particle time-of-flight mass spectrometer described in detail elsewhere.[86] Briefly, particles entering SPLAT II are collimated with an aerodynamic lens inlet that imparts to the particles a velocity that is a function of their vacuum aerodynamic diameter (d_{va}). Particles are detected by two optical detection stages in series (spaced 10.5 cm apart) and sized according to the time between detection events. This time is then used to generate two laser triggers for the pulsed IR laser that causes semivolatile compounds to evaporate from the particle, and, a few microseconds later, the pulsed UV laser that ionizes the evaporated compounds and ablates and ionizes the remaining nonvolatile species. Individual particle mass spectra are acquired with a reflectron time-of-flight mass spectrometer. SPLAT II has a 50% detection cutoff at ~80 nm and can provide information on particle size, composition, density, and morphology.[86−89]

Standards of the ammonium and aminium methanesulfonate salts were prepared separately by mixing MSA (99.0%; Aldrich) with excess 28.7% w/w NH_3 in H_2O (Aldrich), 40% w/w methylamine (MA) in H_2O (Aldrich), 40% w/w dimethylamine (DMA) in H_2O (Aldrich), or 40% w/w trimethylamine (TMA) in H_2O (Aldrich) by adding the basic solution dropwise into a 20 mL vial containing ~5 mL of the acid in an ice bath. These solutions were then dried under vacuum (Spin-Vap; Wheaton) to remove water and excess ammonia or amine. After re-exposure to lab air, some of the salts rapidly and visibly took up water to varying degrees, with MSA-NH_3 taking up the least water and MSA-TMA taking up the most, as is visible in Figure 1. (Salts are referred to as, e.g., MSA-TMA for

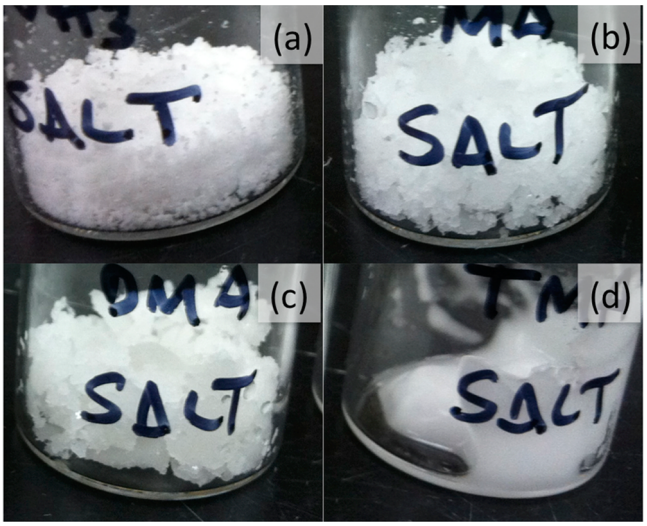

Figure 1. Photographs of salts made from MSA with (a) NH_3, (b) MA, (c) DMA, and (d) TMA showing trend in water uptake at ambient RH.

trimethylaminium methanesulfonate for clarity.) Uptake of water in the case of the MSA-TMA salt was sufficient to quickly yield a viscous brine. These observations are consistent with the reported increase in hygroscopicity going from ammonium to alkylaminium sulfate salts.[90]

Salt standards described above were dissolved in 100 mL Nanopure water (18.1 MΩ, US Filter, Model UHP-10) to make 3−4 mM salt solutions. Note that these concentrations are approximate because the salts had taken up water as described above prior to being weighed. Particles of MSA-NH_3, MSA-MA, MSA-DMA, and MSA-TMA were generated by flowing zero air through a nebulizer (Model 8913; Salter Laboratories) filled with one of the salt solutions. Teflon chambers (~100 L) were filled with zero air until they were ~9 L from being full. The nebulized particles then were added at 3.0 L min^{-1} for ~3 min resulting in ~10:1 dilution of the nebulizer output in the chamber. Assuming the RH of the output of the nebulizer to be 100%, this yields ~10% RH in the chambers.

Gas-phase amine was then added to a Teflon chamber containing particles formed from the nebulized salt solution of MSA and a different amine. The gas-phase displacing amine was generated from standards of MA (10 ppm in N_2; Airgas), DMA (1.4 ppm in N_2; Airgas), or TMA (13.4 ppm in N_2; Matheson) such that its diluted concentration in the chambers was between 350 and 510 ppb (Table 1). It should be noted that these amine concentrations are based on the manufac-

dx.doi.org/10.1021/jp506560w | J. Phys. Chem. C XXXX, XXX, XXX−XXX

Table 1. Initial Conditions and Fraction of Initial Amine Remaining (χ_a) in the Particles for Each Experiment

nebulized salt	displacing amine	initial concentration of the gas-phase amine (ppb)	fraction of initial amine remaining in the particle (χ_a)[a]	reaction time(s) corresponding to χ_a value
MSA-MA	TMA	500	0.32 ± 0.03	overnight
MSA-DMA	TMA	510	0.50 ± 0.05	5 min–overnight
MSA-TMA	MA	500	0.03 ± 0.01	5 min
MSA-TMA	DMA	350	0.02 ± 0.01	5 min

[a]Error calculated based on the 2σ uncertainty in the ionization efficiencies.

turer's stated compressed gas concentrations, which may not be entirely accurate as has been reported previously.[91]

Theoretical Methods. Quantum chemical calculations were carried out to analyze the molecular interactions for the salts formed from MSA with TMA, DMA, MA, and NH_3 in clusters consisting of two acid and two base molecules. Description of such systems requires a method that accurately treats hydrogen bonding, while including significant contributions from dispersion. The choice of the MP2 method with an adequate basis set seems justified for such a case and has been tested against other methods in previous studies.[50,92] Structures were optimized at the MP2 level of theory with the aug-cc-pV(D+d)Z basis set. Harmonic frequencies were calculated to confirm that the structures are minima on the potential surfaces and to estimate the vibrational contribution to enthalpies and free energies of reaction. All calculations were carried out with the Turbomole program package.[93]

RESULTS AND DISCUSSION

Average positive-ion mass spectra normalized to total signal intensity prior to addition of any displacing amine are shown in Figure 2. While mass spectra are presented for MSA-NH_3 salt particles, their low ionization efficiency compared to the amine-containing particles precluded quantification in displacement experiments.

As expected, ions from the methanesulfonate component of the particle are not detected in positive ion mode, but peaks due to NH_4^+ and aminium ions are observed. Thus, in nebulized particles of the three aminium methanesulfonate salts, the dominant peak corresponds to $[M - 1]^+$ for the amines (MA: m/z 30; DMA: m/z 44; TMA: m/z 58) where M is the molar mass of the amine. This is consistent with typical UV ionization MS for alkylamines.[94−96] These peaks are likely due to formation of the amine radical cation followed by loss of ·H to form the corresponding immonium ion $[R_2N{=}CH_2]^+$, as has been shown for the UV ionization of MA and DMA.[94,96] MSA-TMA particles give a significant peak at m/z 42, which may correspond to further loss of ·CH_3 from the $[R_2N{=}CH_2]^+$ species followed by an additional loss of ·H leading to the formation of the $[H_2C{=}N{=}CH_2]^+$ ion, as observed for

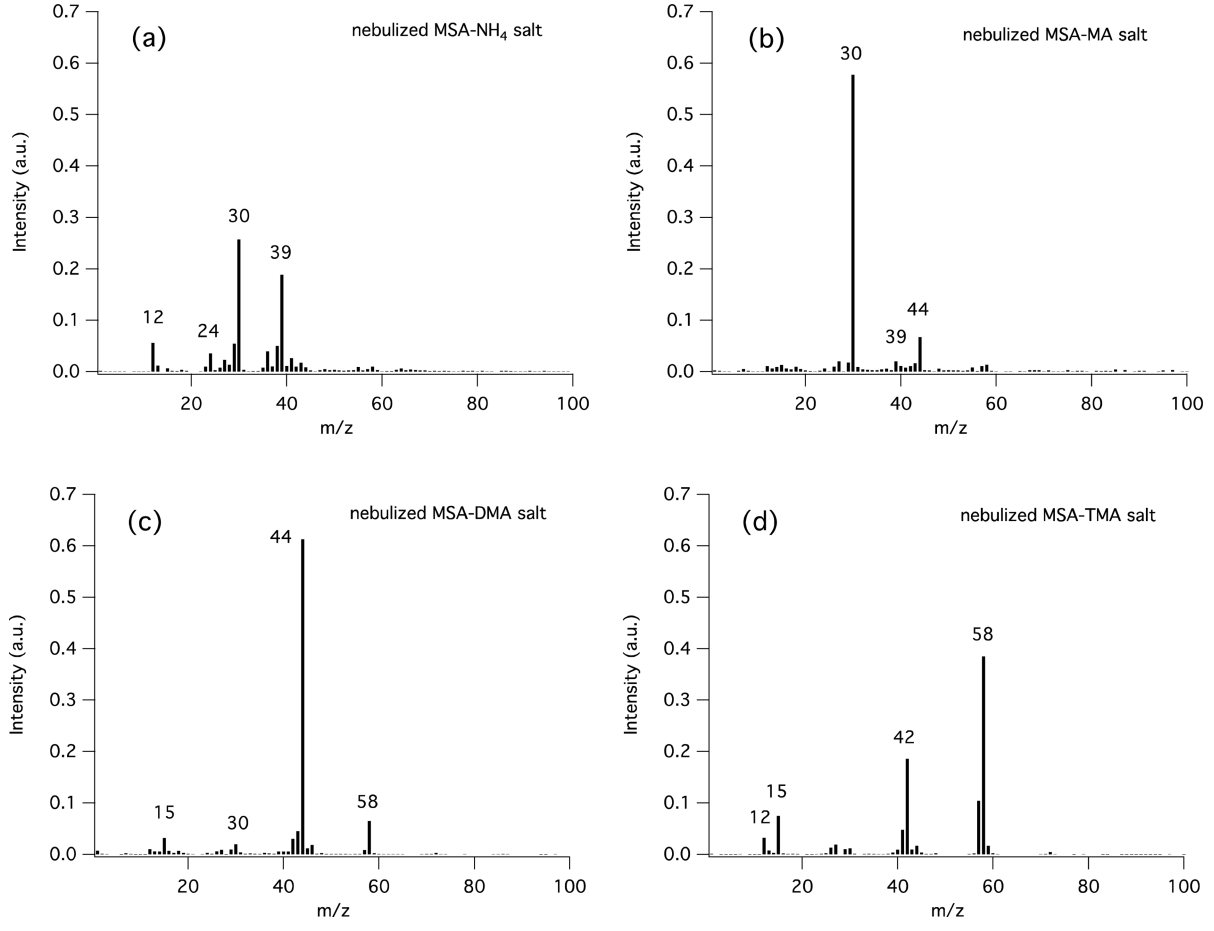

Figure 2. Average positive-ion mass spectra normalized to total signal intensity for particles nebulized from salts made from MSA with (a) NH_3, (b) MA, (c) DMA, and (d) TMA at ∼10% RH.

dx.doi.org/10.1021/jp506560w | J. Phys. Chem. C XXXX, XXX, XXX–XXX

electron impact ionization.[97] For ammonium, methylaminium, and dimethylaminium methanesulfonate particles, peaks corresponding to $[(M-1)+14]^+$ are also present, consistent with fragmentation patterns reported by Angelino and co-workers for particles containing secondary amines such as diethylamine (DEA) and dipropylamine (DPA).[54] Similar to Angelino and co-workers, the $[(M-1)+14]^+$ ion was not observed for trimethylaminium methanesulfonate particles, suggesting a role for the −N−H bond in the formation of this ion.

Size distributions determined by SPLAT-II of particles prior to displacement are shown in Figure 3.[86,88] Little difference is seen between the size distributions of nebulized particles of different compositions. The corresponding SMPS size distributions are shown in Figure S1.

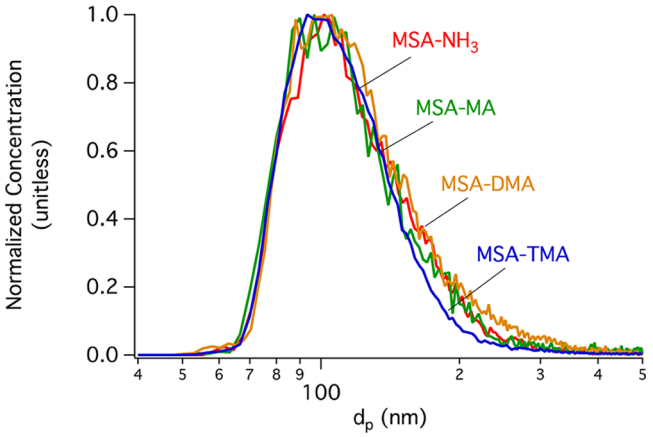

Figure 3. Particle size distributions normalized to peak concentration for particles nebulized from salts made from MSA with NH_3 (red), MA (green), DMA (gold) and TMA (blue) prior to displacement experiments, as measured by SPLAT II. The corresponding SMPS size distributions are shown in Figure S1.

The narrow line-shape of the SPLAT II measured d_{va} size distributions of mobility selected particles shows that all four salts studied here form spherical particles.[89] Particle densities were determined with SPLAT II by measuring the vacuum aerodynamic diameters of mobility classified particles.[89,98] In addition, they were determined using the left edge of the d_{va} size distributions of polydisperse particles measured by SPLAT II[88] and the known SPLAT II characteristic detection efficiency. The two approaches yielded the same values. These data yield the following densities for the nebulized salts, which are MSA-NH_3 $\rho = 1.31 \pm 0.03$ g/cm^3; MSA-MA $\rho = 1.28 \pm 0.03$ g/cm^3; MSA-DMA $\rho = 1.26 \pm 0.03$ g/cm^3; and MSA-TMA $\rho = 1.32 \pm 0.03$ g/cm^3 (2σ). It should be noted, however, that while displacement reactions were carried out at ∼10% RH, the density measurements are based on the size of particles under the low-pressure conditions of the SPLAT II sizing region, where some evaporation of particle-phase water may have taken place.

Figure 4 shows the SPLAT-II size distributions of particles nebulized from salts made from MSA with MA, measured before and after addition of 500 ppb TMA. The addition of a second amine in the gas phase and its interaction with the particles does not change the size distribution. Thus, displacement rather than addition of the gas-phase amine is likely occurring (i.e., the total MA+TMA concentration in the particle-phase remains constant although the concentrations

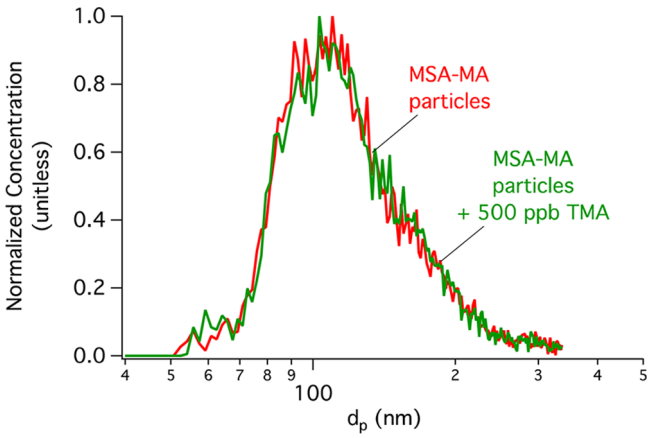

Figure 4. SPLAT-II size distributions normalized to peak concentration for particles nebulized from the salts made from MSA and MA before and after addition of 500 ppb gas-phase TMA.

of the individual N-containing species in the particle-phase change).

To quantify amine−amine displacement, relative ionization efficiencies were calculated for MA, DMA, and TMA. (As mentioned above, the ionization efficiency of NH_3 was too low to use in quantifying displacement). For particles of similar size, the relative total single-particle SPLAT II signal for MSA-MA, MSA-DMA, and MSA-TMA can be used to calculate ionization efficiency. It was found that MSA-TMA particles had the highest ionization efficiency, having a total average signal that was a factor of 2.9 ± 0.4 (2σ) higher than MSA-MA particles, and a factor of 2.1 ± 0.2 (2σ) higher than those of MSA-DMA.

The extent of amine−amine displacement was determined as described in the Supporting Information by monitoring the change in the $[M-1]^+$ peaks for each of the particle-phase amines (MA: m/z 30; DMA: m/z 44; TMA: m/z 58) upon introduction of the gas-phase displacing amine, taking into account the different ionization efficiencies and that some peaks are common to more than one amine. The fraction (χ_a) of the initial amine that remains in the particle phase (i.e., has not been displaced) on exposure to the second amine in the gas phase was calculated for each set of conditions. The initial conditions and final values of χ_a are given in Table 1, along with the reaction times for which the final values of χ_a were calculated. For all but the MSA-MA salt, the reactions were complete within 5 min.

The concentration of added gas-phase displacing amine was in significant excess (>100 times greater) over the initial concentration of particle-phase amine (calculated as the number of particle-phase amine molecules in a given volume of air). Availability of the gas-phase amine will not therefore limit the exchange. As seen from the data in Table 1, essentially complete replacement of the TMA in the MSA-TMA particles occurs when exposed to gas-phase MA or DMA before the first measurement time of ∼5 min. Given that the MSA-TMA salt is much more hygroscopic (Figure 1), the particles are expected to be liquid, with rapid diffusion of gases into and out of the particle, consistent with the rapid, complete displacement observed here.

It is interesting that, despite introducing TMA in great excess, only partial replacement of the particle-phase amine occurs for the MSA-MA and MSA-DMA salts. Replacement of DMA by TMA in the MSA-DMA salt particles is rapid and reaches its final value before the first measurement time of ∼5

dx.doi.org/10.1021/jp506560w | J. Phys. Chem. C XXXX, XXX, XXX−XXX

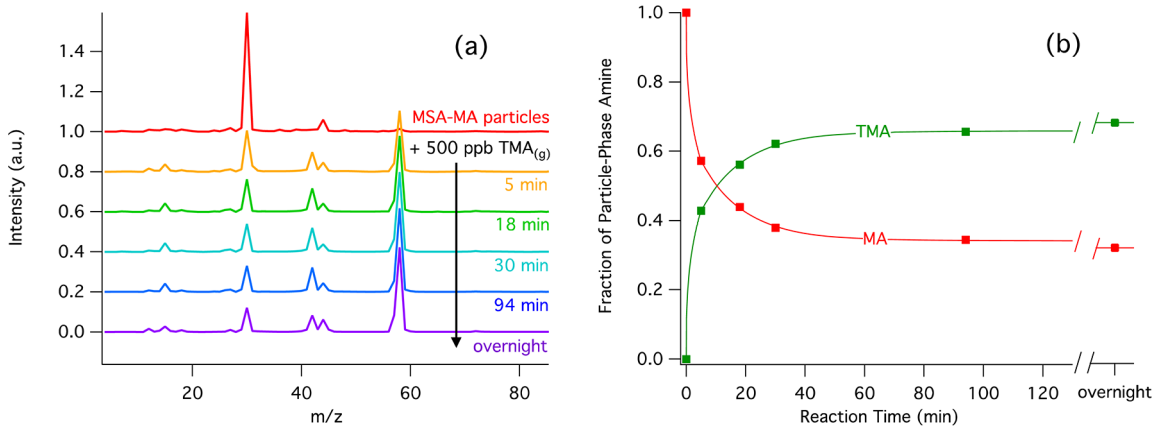

Figure 5. Time resolved (a) SPLAT II mass spectra and (b) χ_{MA} and χ_{TMA}, for the reaction of nebulized MSA-MA salt particles with 500 ppb TMA.

min as was the case for the replacement of TMA by MA and DMA. Values of χ_a for the displacement of DMA by TMA remained unchanged within experimental error from ~5 min reaction time to overnight (Table 1). However, as seen in Figure 5 for the MSA-MA salt, while >40% of the MA was replaced by TMA within 5 min, reaction continued for about an hour, before reaching a final χ_{MA} = 0.32 ± 0.03 overnight (Table 1).

The time dependence observed in the displacement of MA by TMA (Figure 5) indicates that (at least up to ~1 h reaction time) the system is continuing to change. Given that the added gas-phase TMA is in great excess, the lack of complete replacement of the particle-phase amine in the MSA-MA case clearly suggests a limitation to diffusion of incoming TMA through these particles, indicating that MSA-MA particles are not liquid, unlike the MSA-TMA particles. This is also likely the case for displacement of DMA by TMA in MSA-DMA particles, although the time scale is faster than for MSA-MA particles. Similar effects related to particle phase have been seen for amine displacement in $(NH_4)_2SO_4$ particles exposed to triethylamine under various RH conditions.[80,81]

If MSA-MA particles were viscous solids or semisolids, with diffusion in the particle-phase limiting displacement, it would be expected that χ_{MA} would decrease more rapidly for smaller particles. Figure 6 shows the fraction of MSA remaining in the particles as a function of particle size and reaction time, indicating that within experimental error, there is no significant dependence of the extent of replacement on particle size. This suggests that MSA-MA particles cannot be described as simply having one homogeneous, viscous phase. In experiments on displacement of NH_4^+ by DMA in small clusters of NH_4HSO_4, Bzdek et al.[79] show that there is a kinetic limitation to displacement of "core" NH_4^+ molecules compared to those at the surface. Analogously, the larger MSA-MA particles used here could be treated as having a solid, crystalline salt core which does not undergo significant reaction within the time scale of these experiments, buried inside a "shell" of gradually decreasing viscosity which does undergo exchange with the gas phase. Given that the particles are spherical, the data in Figure 6 can be used to estimate the ratio of the approximate effective "shell" thickness (r_{shell}) to the diameter of the particle (d_{va}), assuming the amine densities of the core and shell are the same, and approximating the system as having a clearly defined boundary between the "core" (undisplaced) and "shell" (displaced). Figure 7 shows that this ratio increases with reaction time, approaching 15 ± 6% across all particle sizes after 94 min (purple triangles).

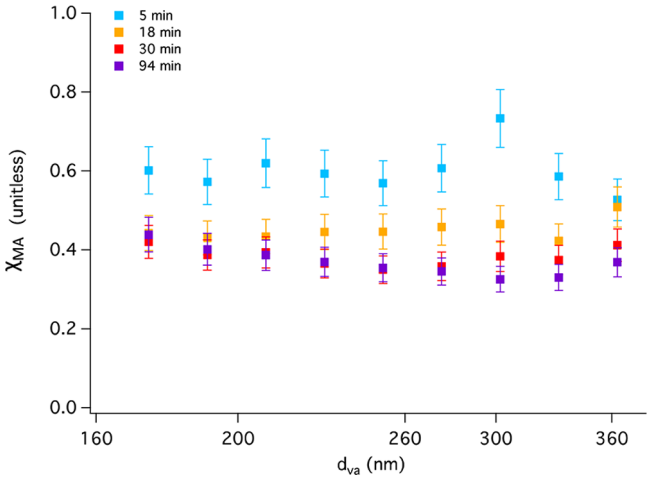

Figure 6. Dependence of χ_{MA} on particle diameter (d_{va}) for the reaction of nebulized MSA-MA salt particles with 500 ppb TMA. Error bars shown are 2σ.

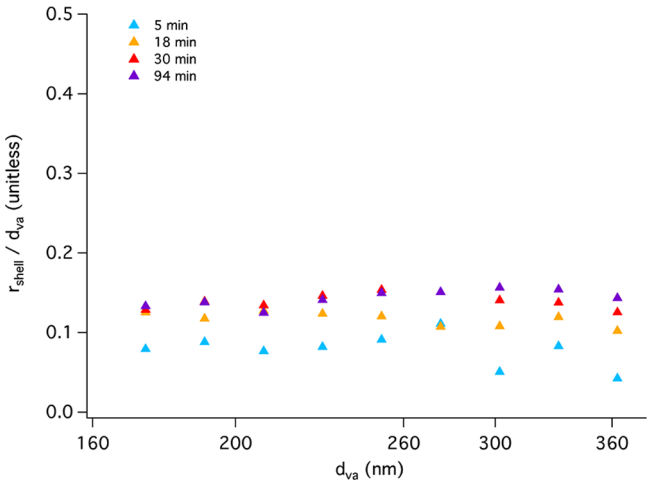

Figure 7. Calculated thickness (r_{shell}) of the displaced portion of each particle relative to its diameter (d_{va}) for the reaction of nebulized MSA-MA salt particles with 500 ppb TMA. This estimate assumes a constant amine density throughout the particle.

dx.doi.org/10.1021/jp506560w | J. Phys. Chem. C XXXX, XXX, XXX–XXX

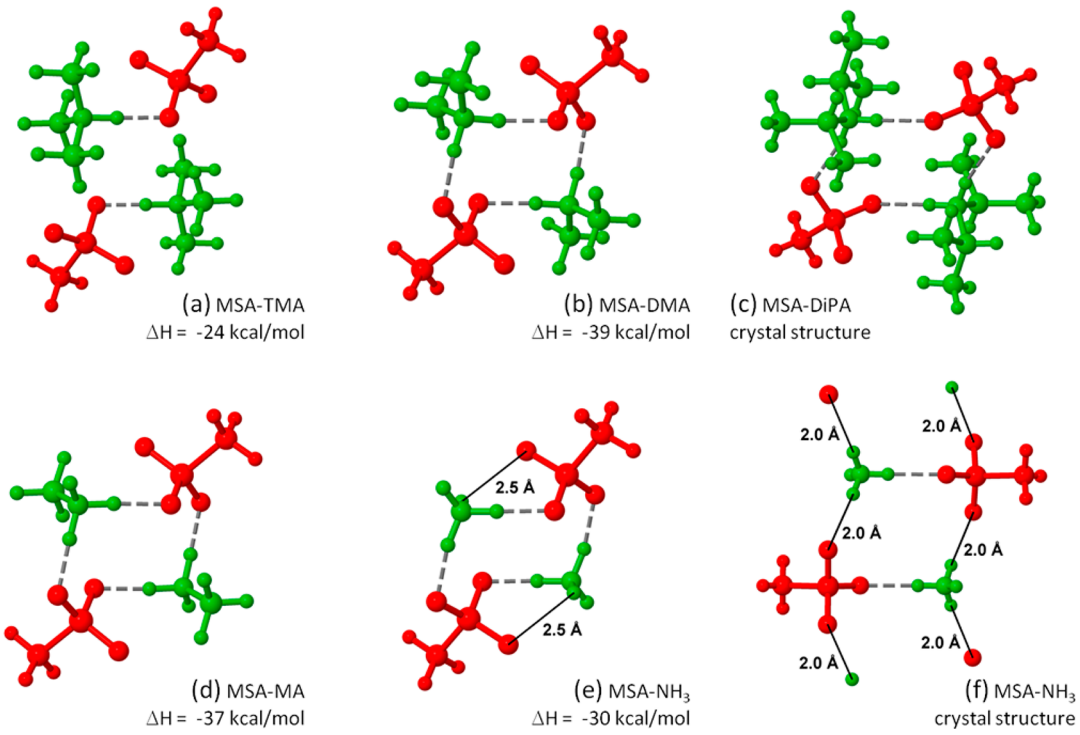

Figure 8. Calculated structures for clusters formed from two MSA and two base molecules, where the base is (a) TMA, (b) DMA, (d) MA and (e) NH_3. Units extracted from the experimental crystal structure of the MSA salt with (c) diisopropylamine (DiPA)[99] and with (f) NH_3[100] are included for comparison. The [amine/ammonia-H^+] cations are colored green and the [$MeSO_3^-$] anions are colored red. Hydrogen bonds with an NH-O distance <2 Å are drawn with a heavy gray dashed line. Additional hydrogen bonding interactions are indicated by solid lines with the NH-O distance. The enthalpies of formation of the [amine/ammonia-H^+]$_2$[$MeSO_3^-$]$_2$ cluster from two [amine/ammonia-H^+][$MeSO_3^-$] ion pairs are included for the predicted structures.

While the 3-D structure of the particles is not known, a more reactive shell on a solid core may arise from the nebulization and drying processes. As the liquid particles from the nebulizer dry under the low RH conditions of the chamber, a solid core of crystalline MSA-MA or MSA-DMA is expected to form, surrounded by an increasingly concentrated salt solution as drying proceeds. The surface layer that ultimately results may contain some water incorporated during the final drying and/or be amorphous rather than crystalline in structure. The salt structure in such a surface layer may then be more easily disrupted by gas-phase TMA than the crystalline core, resulting in a limit to the extent of replacement that can occur on the time scale of these experiments.

To investigate differences in structure and stability that may lead to differences in the interaction of water with the methansulfonate salts as observed in the bulk (Figure 1), as well as the potential for formation of a crystalline core, quantum chemical calculations were carried out on clusters formed from MSA with TMA, DMA, MA and NH_3. Selected structures determined for clusters consisting of two acid and two base molecules are presented in Figure 8. In each acid−base pair, the acidic proton is transferred to the base forming a [amine/ammonia-H^+][$MeSO_3^-$] ion pair. For the fully substituted amine, TMA, there is a hydrogen bond (NH−O distance =1.6 Å) within each ion pair of the [Me_3NH^+]$_2$[$MeSO_3^-$]$_2$ cluster (Figure 8a), but there are no additional −NH groups available for hydrogen bonding between ion pairs. Here we focus on this [Me_3NH^+]$_2$[$MeSO_3^-$]$_2$ cluster with inversion symmetry (C_i) and analogous structures for the other amines to compare to known crystal structures for methanesulfonate salts, but other isomers with similar stability were also identified (see Supporting Information).

The [$Me_2NH_2^+$]$_2$[$MeSO_3^-$]$_2$ cluster (Figure 8b) formed from MSA and DMA has hydrogen bonds within each ion pair and additional hydrogen bonds between neighboring ion pairs. The hydrogen bond distances (NH−O distance =1.7 Å) are slightly longer than in the TMA cluster, but there are a total of four hydrogen bonds compared to two for the TMA cluster. A cyclic hydrogen bonding pattern similar to that of the C_i [$Me_2NH_2^+$]$_2$[$MeSO_3^-$]$_2$ cluster was identified in the experimentally determined crystal structure of the MSA salt with diisopropylamine (DiPA).[99] When the cyclic unit is extracted from the MSA-DiPA crystal structure (Figure 8c) and optimized at the same level of theory as the above clusters, the hydrogen bond distances are shortened (NH−O distance =1.7 Å calculated vs 1.9 Å experimental), but the overall hydrogen bonding pattern remains the same. The similarity between the calculated hydrogen bonding pattern of the C_i [$Me_2NH_2^+$]$_2$[$MeSO_3^-$]$_2$ cluster and the experimentally determined structure of the MSA-DiPA salt suggests that the MSA-DMA salt has a similar stable crystal structure that would resist the uptake of water.

Due to additional −NH groups, the hydrogen bonding networks of [$MeNH_3^+$]$_2$[$MeSO_3^-$]$_2$ (Figure 8d) and [NH_4^+]$_2$[$MeSO_3^-$]$_2$ (Figure 8e), formed from MA and NH_3, respectively, may extend beyond the cyclic structure of these small clusters. An extended hydrogen bonding network was found in the experimentally determined crystal structure for the ammonium methanesulfonate salt (Figure 8f).[100] Alternating cation−anion/anion−cation pairs are stacked, resulting in a laddered structure in which each ion forms a hydrogen bond

dx.doi.org/10.1021/jp506560w | J. Phys. Chem. C XXXX, XXX, XXX−XXX

with three neighbors. As for the MSA-DiPA salt, there is a difference in hydrogen bond distances when comparing the experimental crystal structure (NH−O distance = 1.9 and 2.0 Å) to the calculated structure of the cluster (NH−O distance = 1.7 Å). Here the structure of the cluster is also distorted by rotation of the [$MeSO_3^-$] anion so that the free −SO group is oriented toward a free −NH group. In the solid, the third −SO group would form a hydrogen bond with a neighboring ion pair as shown in Figure 8f. Despite the limitations of the cluster model, the predicted differences in the hydrogen bonding potential of the various amines and the similarities to known crystal structures are useful.

Examination of the gas-phase proton affinities and the fact that TMA is the stronger base suggests that the salt formed from MSA with TMA would be more stable than that formed from MSA with DMA or MA, in contrast with the current experimental results. The calculated ΔH and ΔG values for amine + MSA → [amine-H^+][$MeSO_3^-$] follow the trend for proton affinities (TMA: ΔH = −23 kcal/mol, ΔG = −13 kcal/mol; DMA: ΔH = −21 kcal/mol, ΔG = −9 kcal/mol; MA: ΔH = −18 kcal/mol, ΔG = −7 kcal/mol). However, the interaction energy of two ion pairs, 2 [amine-H^+][$MeSO_3^-$] → [amine-H^+]$_2$[$MeSO_3^-$]$_2$, is significantly greater for the clusters formed from DMA than those formed from TMA due to the hydrogen bonds formed between DMA ion pairs (TMA: ΔH = −24 kcal/mol, ΔG = −11 kcal/mol; DMA: ΔH = −39 kcal/mol, ΔG = −27 kcal/mol). The greater stability of the cluster formed from MSA with DMA is consistent with the experimental result that the MSA-DMA salt is less hygroscopic and the extent of amine displacement is less than for the MSA-TMA salt. The stability of the MSA-MA cluster is similar to, but slightly less than, the stability of the MSA-DMA cluster (MA: ΔH = −37 kcal/mol, ΔG = −25 kcal/mol) since both have the same number of hydrogen bonds in these clusters, but MA is a weaker base. Presumably, the interaction energy of the MA salt will be greater than that of the DMA salt moving beyond the [amine-H^+]$_2$[$MeSO_3^-$]$_2$ cluster size due to additional hydrogen bonds to neighboring ion pairs. Formation of ion pair chains in an extended hydrogen bonding network, as found in the experimental structure of ammonium methanesulfonate salt,[100] may explain the fact that the MA salt undergoes slower replacement than does the DMA salt.

In short, both phase and the nature of the surface layer on solid particles likely determine the time dependence and extent of replacement of one amine in an MSA-amine salt particle with a second one from the gas phase. These displacement reactions may play an important role in aerosol particle growth in the atmosphere in areas where two or more amines are present in the gas-phase. The observed impact of amine species on a particle's physical properties suggest that identifying which amine is present in the particle-phase, and which amines are present in the gas-phase that might displace it, will be necessary to accurately model the evolution of atmospheric aerosol systems.

CONCLUSIONS

Particles formed from MSA and an amine can further interact with a second amine in the gas phase to exchange the particle-phase amine. (An exploration of amine-ammonia exchange was not performed due to the observed low ionization efficiency of ammonium methanesulfonate salt particles.) The extent of displacement by gas-phase amines in particles formed from MSA with MA, DMA, or TMA varies with the amine, likely reflecting different hygroscopicities, and hence phases of the particles, as well as a possible thermodynamic preference. Thus, MSA-TMA particles are highly hygroscopic and expected to be liquid-like even at 10% RH, with essentially complete displacement occurring in the presence of excess MA or DMA. On the other hand, MSA-MA and MSA-DMA particles undergo less displacement by gas-phase TMA, consistent with a solid salt core. Quantum chemical calculations for small clusters of these species indicate that hydrogen-bonding capacity may play a role in the increased water uptake observed for the more substituted MSA-amine species. The observed species-specific effect amines have on particle properties such as hygroscopicity, which in turn affects further growth, makes amine−amine exchange a potentially important reaction in the atmosphere. Understanding these fundamental physical processes involved in displacement reactions is important for predicting the evolution of aerosol systems in the atmosphere and their impacts on health, visibility, and climate.

ASSOCIATED CONTENT

Supporting Information

Included are a derivation of the equation used to calculate the extent of displacement, a figure showing the SMPS particle size distribution for nebulized salts, and additional isomers of the [amine/ammonia-H^+]$_2$[$MeSO_3^-$]$_2$ clusters. This material is available free of charge via the Internet at http://pubs.acs.org.

AUTHOR INFORMATION

Corresponding Authors

*For experiments: bjfinlay@uci.edu; Tel: 949-824-7670; Fax: 949-824-2420.

*For theory: bgerber@uci.edu; Tel 949-824-6758.

Notes

The authors declare no competing financial interest.

ACKNOWLEDGMENTS

The research was performed using EMSL, a national scientific user facility sponsored by the Department of Energy's (DOE) Office of Biological and Environmental Research and located at Pacific Northwest National Laboratory. This work was performed under DOE Grant #ER65208 and NSF Grant #0909227. M.L.D. thanks Metrohm USA and the ARCS Foundation for awards.

REFERENCES

(1) Hinds, W. *Aerosol Technology: Properties, Behavior, and Measurement of Airborne Particles*, 2nd ed.; Wiley-Interscience: New York, 1999.

(2) Michaels, R.; Kleinman, M. Incidence and Apparent Health Significance of Brief Airborne Particle Excursions. *Aerosol Sci. Technol.* **2000**, *32*, 93−105.

(3) Moller, P.; Folkmann, J.; Forchhammer, L.; Brauner, E.; Danielsen, P.; Risom, L.; Loft, S. Air Pollution, Oxidative Damage to DNA, and Carcinogenesis. *Cancer Lett.* **2008**, *266*, 84−97.

(4) Pope, C. A.; Muhlestein, J. B.; May, H. T.; Renlund, D. G.; Anderson, J. L.; Horne, B. D. Ischemic Heart Disease Events Triggered by Short-Term Exposure to Fine Particulate Air Pollution. *Circulation* **2006**, *114*, 2443−2448.

(5) Pope, C. A., III; Dockery, D. W. Health Effects of Fine Particulate Air Pollution: Lines that Connect. *J. Air Waste Manage. Assoc.* **2006**, *56*, 709−742.

(6) Colbeck, I.; Lazaridis, M. Aerosols and Environmental Pollution. *Naturwissenschaften* **2010**, *97*, 117−131.

(7) Finlayson-Pitts, B. J.; Pitts, J. N. *Chemistry of the Upper and Lower Atmosphere – Theory, Experiments and Applications*; Academic Press: San Diego, CA, 2000.
(8) *IPCC, 2013: Climate Change 2013: The Physical Science Basis. Contribution of Working Group 1 to the Fifth Assessment Report of the Intergovernmental Panel on Climate Change*; Cambridge University Press: Cambridge, U.K. and New York, p 1535.
(9) Andreae, M. O.; Rosenfeld, D. Aerosol-Cloud-Precipitation Interactions. Part 1. The Nature and Sources of Cloud-Active Aerosols. *Earth-Sci. Rev.* **2008**, *89*, 13–41.
(10) Kulmala, M.; Vehkamäki, H.; Petäjä, T.; Dal Maso, M.; Lauri, A.; Kerminen, V.-M.; Birmili, W.; McMurry, P. H. Formation and Growth Rates of Ultrafine Atmospheric Particles: A Review of Observations. *J. Aerosol Sci.* **2004**, *35*, 143–176.
(11) Bzdek, B. R.; Johnston, M. V. New Particle Formation and Growth in the Troposphere. *Anal. Chem.* **2010**, *82*, 7871–7878.
(12) Zhang, R.; Khalizov, A.; Wang, L.; Hu, M.; Xu, W. Nucleation and Growth of Nanoparticles in the Atmosphere. *Chem. Rev.* **2012**, *112*, 1957–2011.
(13) Smith, J.; Barsanti, K.; Friedli, H.; Ehn, M.; Kulmala, M.; Collins, D.; Scheckman, J.; Williams, B.; McMurry, P. Observations of Aminium Salts in Atmospheric Nanoparticles and Possible Climatic Implications. *Proc. Natl. Acad. Sci. U.S.A.* **2010**, *107*, 6634–6639.
(14) Kulmala, M.; Kerminen, V. On the Formation and Growth of Atmospheric Nanoparticles. *Atmos. Res.* **2008**, *90*, 132–150.
(15) Facchini, M. C.; Decesari, S.; Rinaldi, M.; Carbone, C.; Finessi, E.; Mircea, M.; Fuzzi, S.; Moretti, F.; Tagliavini, E.; Ceburnis, D.; et al. Important Source of Marine Secondary Organic Aerosol from Biogenic Amines. *Environ. Sci. Technol.* **2008**, *42*, 9116–9121.
(16) Muller, C.; Iinuma, Y.; Karstensen, J.; van Pinxteren, D.; Lehmann, S.; Gnauk, T.; Herrmann, H. Seasonal Variation of Aliphatic Amines in Marine Sub-micrometer Particles at the Cape Verde Islands. *Atmos. Chem. Phys.* **2009**, *9*, 9587–9597.
(17) Bardouki, H.; Berresheim, H.; Vrekoussis, M.; Sciare, J.; Kouvarakis, G.; Oikonomou, K.; Schneider, J.; Mihalopoulos, N. Gaseous (DMS, MSA, SO_2, H_2SO_4 and DMSO) and Particulate (Sulfate and Methanesulfonate) Sulfur Species over the Northeastern Coast of Crete. *Atmos. Chem. Phys.* **2003**, *3*, 1871–1886.
(18) Berresheim, H.; Elste, T.; Tremmel, H.; Allen, A.; Hansson, H.; Rosman, K.; Dal Maso, M.; Makela, J. M.; Kulmala, M.; O'Dowd, C. D. Gas-Aerosol Relationships of H_2SO_4, MSA, and OH: Observations in the Coastal Marine Boundary Layer at Mace Head, Ireland. *J. Geophys. Res. - Atmos* **2002**, DOI: 10.1029/2000JD000229.
(19) Chen, L.; Wang, J.; Gao, Y.; Xu, G.; Yang, X.; Lin, Q.; Zhang, Y. Latitudinal Distributions of Atmospheric MSA and MSA/nss-SO_4^{2-} Ratios in Summer over the High Latitude Regions of the Southern and Northern Hemispheres. *J. Geophys. Res. - Atmos* **2012**, DOI: 10.1029/2011JD016559.
(20) Sorooshian, A.; Padro, L. T.; Nenes, A.; Feingold, G.; McComiskey, A.; Hersey, S. P.; Gates, H.; Jonsson, H. H.; Miller, S. D.; Stephens, G. L.; et al. On the Link Between Ocean Biota Emissions, Aerosol, and Maritime Clouds: Airborne, Ground, and Satellite Measurements off the coast of California. *Global Biogeochem. Cycles* **2009**, DOI: 10.1029/2009GB003464.
(21) Berresheim, H.; Huey, J. W.; Thorn, R. P.; Eisele, F. L.; Tanner, D. J.; Jefferson, A. Measurements of Dimethyl Sulfide, Dimethyl Sulfoxide, Dimethyl Sulfone, and Aerosol Ions at Palmer Station, Antarctica. *J. Geophys. Res. - Atmos* **1998**, *103*, 1629–1637.
(22) Makela, J. M.; Yli-Koivisto, S.; Hiltunen, V.; Seidl, W.; Swietlicki, E.; Teinila, K.; Sillanpaa, M.; Koponen, I. K.; Paatero, J.; Rosman, K.; et al. Chemical Composition of Aerosol During Particle Formation Events in Boreal Forest. *Tellus, Ser. B* **2001**, *53*, 380–393.
(23) Kerminen, V.; Aurela, M.; Hillamo, R.; Virkkula, A. Formation of Particulate MSA: Deductions from Size Distribution Measurements in the Finnish Arctic. *Tellus, Ser. B* **1997**, *49*, 159–171.
(24) Barnes, I.; Becker, K. H.; Mihalopoulos, N. An FTIR Product Study of the Photooxidation of Dimethyl Disulfide. *J. Atmos. Chem.* **1994**, *18*, 267–289.
(25) Hatakeyama, S.; Okuda, M.; Akimoto, H. Formation of Sulfur-Dioxide and Methanesulfonic-Acid in the Photo-Oxidation of Dimethyl Sulfide in the Air. *Geophys. Res. Lett.* **1982**, *9*, 583–586.
(26) Yin, F.; Grosjean, D.; Flagan, R. C.; Seinfeld, J. H. Photooxidation of Dimethyl Sulfide and Dimethyl Disulfide. II: Mechanism Evaluation. *J. Atmos. Chem.* **1990**, *11*, 365–399.
(27) Yin, F.; Grosjean, D.; Seinfeld, J. H. Photooxidation of Dimethyl Sulfide and Dimethyl Disulfide. I: Mechanism Development. *J. Atmos. Chem.* **1990**, *11*, 309–364.
(28) Dingenen, R.; Jensen, N. R.; Hjorth, J.; Raes, F. Peroxynitrate Formation During the Night-Time Oxidation of Dimethylsulfide: Its Role as a Reservoir Species for Aerosol Formation. *J. Atmos. Chem.* **1994**, *18*, 211–237.
(29) Tyndall, G. S.; Ravishankara, A. R. Atmospheric Oxidation of Reduced Sulfur Species. *Int. J. Chem. Kinet.* **1991**, *23*, 483–527.
(30) Zhu, L.; Nenes, A.; Wine, P. H.; Nicovich, J. M. Effects of Aqueous Organosulfur Chemistry on Particulate Methanesulfonate to Non–Sea Salt Sulfate Ratios in the Marine Atmosphere. *J. Geophys. Res. - Atmos* **2006**, DOI: 10.1029/2005JD006326.
(31) Capaldo, K. P.; Pandis, S. N. Dimethylsulfide Chemistry in the Remote Marine Atmosphere: Evaluation and Sensitivity Analysis of Available Mechanisms. *J. Geophys. Res. - Atmos* **1997**, *102*, 23251–23267.
(32) Patroescu, I. V.; Barnes, I.; Becker, K. H.; Mihalopoulos, N. FT-IR Product Study of the OH-Initiated Oxidation of DMS in the Presence of NO_x. *Atmos. Environ.* **1998**, *33*, 25–35.
(33) Chen, T.; Jang, M. Secondary Organic Aerosol Formation from Photooxidation of a Mixture of Dimethyl Sulfide and Isoprene. *Atmos. Environ.* **2012**, *46*, 271–278.
(34) Bates, T.; Lamb, B.; Guenther, A.; Dignon, J.; Stoiber, R. Sulfur Emissions to the Atmosphere from Natural Sources. *J. Atmos. Chem.* **1992**, *14*, 315–337.
(35) Kettle, A.; Andreae, M. Flux of Dimethylsulfide from the Oceans: A Comparison of Updated Data Seas and Flux Models. *J. Geophys. Res. - Atmos* **2000**, *105*, 26793–26808.
(36) Kettle, A.; Rhee, T.; von Hobe, M.; Poulton, A.; Aiken, J.; Andreae, M. Assessing the Flux of Different Volatile Sulfur Gases from the Ocean to the Atmosphere. *J. Geophys. Res. - Atmos* **2001**, *106*, 12193–12209.
(37) Yvon, S.; Saltzman, E.; Cooper, D.; Bates, T.; Thompson, A. Atmospheric Sulfur Cycling in the Tropical Pacific Marine Boundary Layer (12°S,135°W): A Comparison of Field Data and Model Results. 1. Dimethylsulfide. *J. Geophys. Res. - Atmos* **1996**, *101*, 6899–6909.
(38) Andreae, M.; Raemdonck, H. Dimethyl Sulfide in the Surface Ocean and the Marine Atmosphere - A Global View. *Science* **1983**, *221*, 744–747.
(39) Andreae, M. O.; Ferek, R. J.; Bermond, F.; Byrd, K. P.; Engstrom, R. T.; Hardin, S.; Houmere, P. D.; LeMarrec, F.; Raemdonck, H.; Chatfield, R. B. Dimethyl Sulfide in the Marine Atmosphere. *J. Geophys. Res. - Atmos* **1985**, *90*, 2891–2900.
(40) Feilberg, A.; Liu, D.; Adamsen, A. P. S.; Hansen, M. J.; Jonassen, K. E. N. Odorant Emissions from Intensive Pig Production Measured by Online Proton-Transfer-Reaction Mass Spectrometry. *Environ. Sci. Technol.* **2010**, *44*, 5894–5900.
(41) Filipy, J.; Rumburg, B.; Mount, G.; Westberg, H.; Lamb, B. Identification and Quantification of Volatile Organic Compounds from a Dairy. *Atmos. Environ.* **2006**, *40*, 1480–1494.
(42) Gay, S.; Schmidt, D.; Clanton, C.; Janni, K.; Jacobson, L.; Weisberg, S. Odor, Total Reduced Sulfur, and Ammonia Emissions from Animal Housing Facilities and Manure Storage Units in Minnesota. *Appl. Eng. Agric.* **2003**, *19*, 347–360.
(43) Kim, K.-H. Emissions of Reduced Sulfur Compounds (RSC) as a Landfill Gas (LFG): A Comparative Study of Young and Old Landfill Facilities. *Atmos. Environ.* **2006**, *40*, 6567–6578.
(44) Kim, K.-H.; Jeon, E.-C.; Koo, Y.-S.; Im, M.-S.; Youn, Y.-H. An On-Line Analysis of Reduced Sulfur Gases in the Ambient Air Surrounding a Large Industrial Complex. *Atmos. Environ.* **2007**, *41*, 3829–3840.

(45) Lunn, F.; Van de Vyver, J. Sampling and Analysis of Air in Pig Houses. *Agr. Environ.* **1977**, *3*, 159−169.
(46) Ge, X.; Zhang, Q.; Sun, Y.; Ruehl, C. R.; Setyan, A. Effect of Aqueous-Phase Processing on Aerosol Chemistry and Size Distriutions in Fresno, California, During Wintertime. *Environ. Chem.* **2012**, *9* (3), 221−235.
(47) Kreidenweis, S.; Flagan, R.; Seinfeld, J.; Okuyama, K. Binary Nucleation of Methanesulfonic Acid and Water. *J. Aerosol Sci.* **1989**, *20*, 585−607.
(48) Wyslouzil, B.; Seinfeld, J.; Flagan, R.; Okuyama, K. Binary Nucleation in Acid-Water Systems 1. Methanesulfonic Acid−Water. *J. Chem. Phys.* **1991**, *94*, 6827−6841.
(49) Wyslouzil, B.; Seinfeld, J.; Flagan, R.; Okuyama, K. Binary Nucleation in Acid-Water Systems 2. Sulfuric Acid−Water and a Comparison with Methanesulfonic Acid−Water. *J. Chem. Phys.* **1991**, *94*, 6842−6850.
(50) Dawson, M. L.; Varner, M. E.; Perraud, V.; Ezell, M. J.; Gerber, R. B.; Finlayson-Pitts, B. J. Simplified Mechanism for New Particle Formation from Methanesulfonic Acid, Amines, and Water via Experiments and *ab initio* Calculations. *Proc. Natl. Acad. Sci. U. S. A.* **2012**, *109*, 18719−18724.
(51) Ge, X.; Wexler, A.; Clegg, S. Atmospheric Amines - Part I. A Review. *Atmos. Environ.* **2011**, *45*, 524−546.
(52) Anderson, N.; Strader, R.; Davidson, C. Airborne Reduced Nitrogen: Ammonia Emissions from Agriculture and Other Sources. *Environ. Int.* **2003**, *29*, 277−286.
(53) Jickells, T.; Baker, A. R.; Cape, J. N.; Cornell, S. E.; Nemitz, E. The Cycling of Organic Nitrogen Through the Atmosphere. *Philos. Trans. R. Soc. B* **2013**, *368*, 20130115.
(54) Angelino, S.; Suess, D.; Prather, K. Formation of Aerosol Particles from Reactions of Secondary and Tertiary Alkylamines: Characterization by Aerosol Time-of-Flight Mass Spectrometry. *Environ. Sci. Technol.* **2001**, *35*, 3130−3138.
(55) Berndt, T.; Stratmann, F.; Sipila, M.; Vanhanen, J.; Petaja, T.; Mikkila, J.; Gruner, A.; Spindler, G.; Mauldin, R. L.; Curtius, J.; et al. Laboratory Study on New Particle Formation from the Reaction OH + SO_2: Influence of Experimental Conditions, H_2O Vapour, NH_3 and the Amine *tert*-Butylamine on the Overall Process. *Atmos. Chem. Phys.* **2010**, *10*, 7101−7116.
(56) Kirkby, J.; Curtius, J.; Almeida, J.; Dunne, E.; Duplissy, J.; Ehrhart, S.; Franchin, A.; Gagne, S.; Ickes, L.; Kuerten, A.; et al. Role of Sulphuric Acid, Ammonia and Galactic Cosmic Rays in Atmospheric Aerosol Nucleation. *Nature* **2011**, *476*, 429−433.
(57) Yu, H.; McGraw, R.; Lee, S.-H. Effects of Amines on Formation of Sub-3 nm Particles and Their Subsequent Growth. *Geophys. Res. Lett.* **2012**, DOI: 10.1029/2011GL050099.
(58) Zollner, J. H.; Glasoe, W. A.; Panta, B.; Carlson, K. K.; McMurry, P. H.; Hanson, D. R. Sulfuric Acid Nucleation: Power Dependencies, Variation with Relative Humidity, and Effect of Bases. *Atmos. Chem. Phys.* **2012**, *12*, 4399−4411.
(59) Kurten, T.; Loukonen, V.; Vehkamaki, H.; Kulmala, M. Amines are Likely to Enhance Neutral and Ion-Induced Sulfuric Acid−Water Nucleation in the Atmosphere More Effectively than Ammonia. *Atmos. Chem. Phys.* **2008**, *8*, 4095−4103.
(60) Loukonen, V.; Kuo, I.-F. W.; McGrath, M. J.; Vehkamäki, H. On the Stability and Dynamics of (Sulfuric Acid) (Ammonia) and (Sulfuric Acid) (Dimethylamine) Clusters: A First-Principles Molecular Dynamics Investigation. *Chem. Phys.* **2014**, *428*, 164−174.
(61) Berndt, T.; Sipilä, M.; Stratmann, F.; Petäjä, T.; Vanhanen, J.; Mikkilä, J.; Patokoski, J.; Taipale, R.; Mauldin, R. L., III; Kulmala, M. Enhancement of Atmospheric H_2SO_4/H_2O Nucleation: Organic Oxidation Products Versus Amines. *Atmos. Chem. Phys.* **2014**, *14*, 751−764.
(62) Almeida, J.; Schobesberger, S.; Kürten, A.; Ortega, I. K.; Kupiainen-Määttä, O.; Praplan, A. P.; Adamov, A.; Amorim, A.; Bianchi, F.; Breitenlechner, M.; et al. Molecular Understanding of Sulphuric Acid-Amine Particle Nucleation in the Atmosphere. *Nature* **2013**, *502*, 359−363.
(63) Cablk, M. E.; Szelagowski, E. E.; Sagebiel, J. C. Characterization of the Volatile Organic Compounds Present in the Headspace of Decomposing Animal Remains, and Compared with Human Remains. *Forensic Sci. Int.* **2012**, *220*, 118−125.
(64) Kuhn, U.; Sintermann, J.; Spirig, C.; Jocher, M.; Ammann, C.; Neftel, A. Basic Biogenic Aerosol Precursors: Agricultural Source Attribution of Volatile Amines Revised. *Geophys. Res. Lett.* **2011**, DOI: 10.1029/2011GL047958.
(65) Mosier, A.; Andre, C.; Viets, F. Identification of Aliphatic Amines Volatilized from Cattle Feedyard. *Environ. Sci. Technol.* **1973**, *7*, 642−644.
(66) Schade, G.; Crutzen, P. Emission of Aliphatic Amines from Animal Husbandry and Their Reactions: Potential Source of N_2O and HCN. *J. Atmos. Chem.* **1995**, *22*, 319−346.
(67) Fujii, T.; Kitai, T. Determination of Trace Levels of Trimethylamine in Air by Gas Chromatography/Surface Ionization Organic Mass Spectrometry. *Anal. Chem.* **1987**, *59*, 379−382.
(68) Hutchinson, G. L.; Mosier, A. R.; Andre, C. E. Ammonia and Amine Emissions from a Large Cattle Feedlot. *J. Environ. Qual.* **1982**, *11*, 288.
(69) Akyüz, M. Simultaneous Determination of Aliphatic and Aromatic Amines in Ambient Air and Airborne Particulate Matter by Gas Chromatography-Mass Spectrometry. *Atmos. Environ.* **2008**, *42*, 3809−3819.
(70) Lobert, J. M.; Scharffe, D. H.; Hao, W. M.; Crutzen, P. J. Importance of Biomass Burning in the Atmospheric Budgets of Nitrogen-Containing Gases. *Nature* **1990**, *346*, 552−554.
(71) Nielsen, C. J.; Herrmann, H.; Weller, C. Atmospheric Chemistry and Environmental Impact of the Use of Amines in Carbon Capture and Storage (CCS). *Chem. Soc. Rev.* **2012**, *41*, 6684−6704.
(72) Rochelle, G. T. Amine Scrubbing for CO_2 Capture. *Science* **2009**, *325*, 1652−1654.
(73) Schreiber, A.; Zapp, P.; Kuckshinrichs, W. Environmental Assessment of German Electricity Generation from Coal-Fired Power Plants with Amine-Based Carbon Capture. *Int. J. Life Cycle Assess.* **2009**, *14*, 547−559.
(74) Ge, X.; Shaw, S. L.; Zhang, Q. Toward Understanding Amines and Their Degradation Products from Precombustion CO_2 Capture Processes with Aerosol Mass Spectrometry. *Environ. Sci. Technol.* **2014**, *48* (9), 5066−5075.
(75) Barsanti, K. C.; McMurry, P. H.; Smith, J. N. The Potential Contribution of Organic Salts to New Particle Growth. *Atmos. Chem. Phys.* **2009**, *9*, 2949−2957.
(76) Erupe, M. E.; Viggiano, A. A.; Lee, S.-H. The Effect of Trimethylamine on Atmospheric Nucleation Involving H_2SO_4. *Atmos. Chem. Phys.* **2011**, *11*, 4767−4775.
(77) Bzdek, B. R.; Ridge, D. P.; Johnston, M. V. Amine Exchange into Ammonium Bisulfate and Ammonium Nitrate Nuclei. *Atmos. Chem. Phys.* **2010**, *10*, 3495−3503.
(78) Bzdek, B. R.; Ridge, D. P.; Johnston, M. V. Reactivity of Methanesulfonic Acid Salt Clusters Relevant to Marine Air. *J. Geophys. Res. - Atmos* **2011**, DOI: 10.1029/2010JD015217.
(79) Bzdek, B. R.; Ridge, D. P.; Johnston, M. V. Size-Dependent Reactions of Ammonium Bisulfate Clusters with Dimethylamine. *J. Phys. Chem. A* **2010**, *114*, 11638−11644.
(80) Chan, L. P.; Chan, C. K. Displacement of Ammonium from Aerosol Particles by Uptake of Triethylamine. *Aerosol Sci. Technol.* **2012**, *46*, 236−247.
(81) Chan, L. P.; Chan, C. K. Role of the Aerosol Phase State in Ammonia/Amines Exchange Reactions. *Environ. Sci. Technol.* **2013**, *47*, 5755−5762.
(82) Lloyd, J.; Heaton, K.; Johnston, M. Reactive Uptake of Trimethylamine into Ammonium Nitrate Particles. *J. Phys. Chem. A* **2009**, *113*, 4840−4843.
(83) Liu, Y.; Han, C.; Liu, C.; Ma, J.; Ma, Q.; He, H. Differences in the Reactivity of Ammonium Salts with Methylamine. *Atmos. Chem. Phys.* **2012**, *12*, 4855−4865.

(84) Qiu, C.; Wang, L.; Lal, V.; Khalizov, A. F.; Zhang, R. Heterogeneous Reactions of Alkylamines with Ammonium Sulfate and Ammonium Bisulfate. *Environ. Sci. Technol.* **2011**, *45*, 4748−4755.
(85) Murphy, S. M.; Sorooshian, J. H.; Kroll, J. H.; Ng, N. L.; Chhabra, P.; Tong, C.; Surratt, J. D.; Knipping, E.; Flagan, R. C.; Seinfeld, J. H. Secondary Aerosol Formation from Atmospheric Reactions of Aliphatic Amines. *Atmos. Chem. Phys.* **2007**, *7*, 2313−2337.
(86) Zelenyuk, A.; Yang, J.; Choi, E.; Imre, D. SPLAT II: An Aircraft Compatible, Ultra-Sensitive, High Precision Instrument for *in-situ* Characterization of the Size and Composition of Fine and Ultrafine Particles. *Aerosol Sci. Technol.* **2009**, *43*, 411−424.
(87) Vaden, T. D.; Imre, D.; Beranek, J.; Zelenyuk, A. Extending the Capabilities of Single Particle Mass Spectrometry: I. Measurements of Aerosol Number Concentration, Size Distribution, and Asphericity. *Aerosol Sci. Technol.* **2011**, *45*, 113−124.
(88) Vaden, T. D.; Imre, D.; Beranek, J.; Zelenyuk, A. Extending the Capabilities of Single Particle Mass Spectrometry: II. Measurements of Aerosol Particle Density without DMA. *Aerosol Sci. Technol.* **2011**, *45*, 125−135.
(89) Zelenyuk, A.; Yang, J.; Song, C.; Zaveri, R. A.; Imre, D. A New Real-Time Method for Determining Particles' Sphericity and Density: Application to Secondary Organic Aerosol Formed by Ozonolysis of α-Pinene. *Environ. Sci. Technol.* **2008**, *42*, 8033−8038.
(90) Hu, D.; Li, C.; Chen, H.; Chen, J.; Ye, X.; Li, L.; Yang, X.; Wang, X.; Mellouki, A.; Hu, Z. Hygroscopicity and Optical Properties of Alkylaminium Sulfates. *J. Environ. Sci.* **2014**, *26*, 37−43.
(91) Dawson, M. L.; Perraud, V.; Gomez, A.; Arquero, K. D.; Ezell, M.; Finlayson-Pitts, B. J. Measurement of Gas-Phase Ammonia and Amines in Air by Collection onto an Ion Exchange Resin and Analysis by Ion Chromatography. *Atmos. Meas. Tech.* **2014**, *7*, 2733−2744.
(92) Ortega, I. K.; Kupiainen, O.; Kurten, T.; Olenius, T.; Wilkman, O.; McGrath, M. J.; Loukonen, V.; Vehkamaki, H. From Quantum Chemical Formation Free Energies to Evaporation Rates. *Atmos. Chem. Phys.* **2012**, *12*, 225−235.
(93) TURBOMOLE V6.5 2013, a development of University of Karlsruhe and Forschungszentrum Karlsruhe GmbH, 1989−2007, TURBOMOLE GmbH, since 2007; available from http://www.turbomole.com.
(94) Jie, W.; Bing, Z.; Li, F.; Wenyue, G.; Liandi, Z.; Shudong, Z.; Jiye, C. Multiphoton Ionization of Ethylamine and Dimethylamine Enhanced by Resonance Excitation to the 3s Rydberg State. *Acta Physico-Chimica Sinica* **1997**, *13*, 732−735.
(95) Siuzdak, G.; BelBruno, J. J. Multiphoton Ionization Studies of Amines with UV-VIS Lasers. *Appl. Phys. B: Laser Opt.* **1990**, *50*, 221−226.
(96) Xiaojun, L.; Bing, Z.; Li, F.; Wenyue, G.; Jingang, Z.; Jiye, C.; Yiqun, L.; Shikang, Z. Study of the Multiphoton Ionization Mass Spectra Methylamine. *Acta Phys.-Chim. Sin.* **1996**, *12*, 981−985.
(97) Hvistendahl, G.; Undheim, K. High Resolution Mass Spectrometry of Trimethylamine. *Org. Mass Spectrom.* **1970**, *3*, 821−824.
(98) Zelenyuk, A.; Cai, Y.; Chieffo, L.; Imre, D. High Precision Density Measurements of Single Particles: The Density of Metastable Phases. *Aerosol Sci. Technol.* **2005**, *39* (10), 972−986.
(99) Reiss, G. J.; Meyer, M. K. Diisopropylammonium Methanesulfonate. *Acta Crystallogr., Sect. E: Struct. Rep. Online* **2011**, *67*, 2169.
(100) Wei, C. H. Structure of Ammonium Methanesulfonate. *Acta Cryst. C* **1986**, *42* (12), 1839−1842.